SUPPORTING INFORMATION

SI 1. Meteorology

Back trajectories of the air masses arriving at the measurement site were calculated for 00:00 and 12:00 for each day of the campaign, depicting the path taken by the air mass reaching the sampling site over the previous five days. The back trajectories were run using the on-line HYSPLIT model developed by the National Oceanic and Atmospheric Administration (NOAA) (Draxler and Rolph, 2003).

Three predominant origins of air masses arriving at the receptor were classified. Marine Polar (mP) described air masses emerging from polar regions around southern Greenland and advecting south-east over the North Atlantic, marine Arctic (mA) air coming mainly form the north Scandanavian Arctic regions and Continental marine polar (cmP) for air stagnated as a pressure gradually strengthened and centered over Mace Head and anti-cyclonic conditions were observed for most of the time during this period.

Days (February 2009)	Air mass type	Cold Marine	Stagnant
1st	cmP		V
2nd, 3rd	cP		V
4th	cmP		V
5th – 8th	mA	V	
9th -15th	mP	V	
16th -19th	cmP		V
20th -22nd	mP	V	

Table S1. Air mass back trajectories.

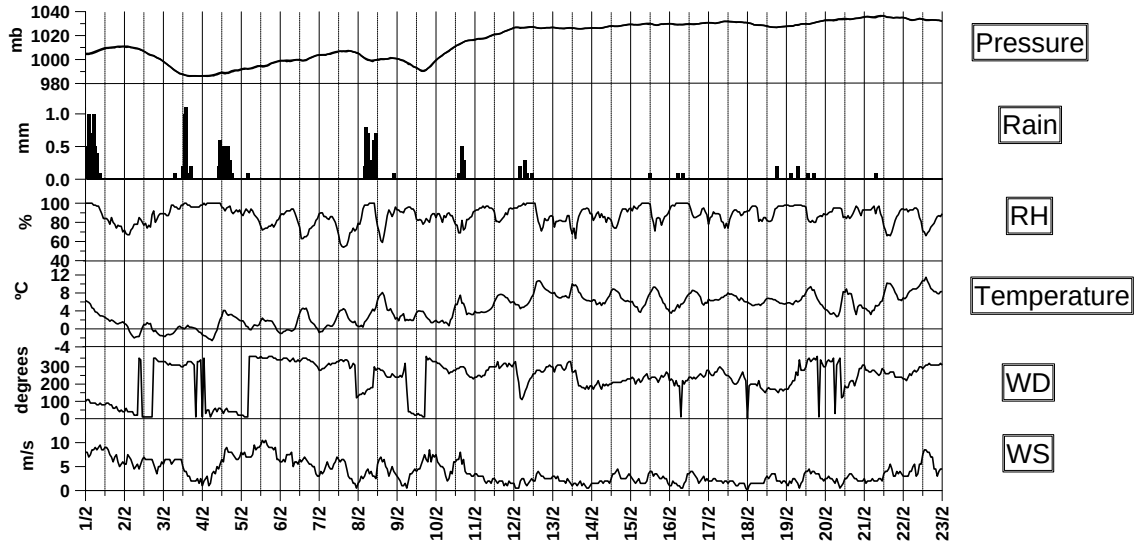

Fig. S1: Summary of local meteorological parameters.

SI 2. Correlation table for AMS (Table S2) and ATOFMS (Table S3) between aerosol categories and selected m/z peaks

ATOFMS	***OC-EC-SUL***	***OC-EC-NIT***	***OC-EC-CH***	***Na-K-OC-NIT***	***Ca-EC***
m/z 113	0.52	<0.1	**0.65**	0.30	0.11
m/z 37	**0.94**	0.30	**0.74**	0.48	0.14
m/z 55	**0.76**	<0.1	**0.70**	<0.1	0.14

Table S2. Correlation table between selected ATOFMS peaks (m/z 37, 55 and 113) and organic main ATOFMS particle types. Correlations were obtained by temporal series of ATOFMS clusters and ATOFMS peaks queries from the dataset.

m/z	*Species*	*AMS Factor*				
		1	***2***	***3***	***4***	***5***
		LV-OOA	***COA***	***HOA***	***PCOA***	***BBOA***
29	C_2H_5	0.21	**0.65**	0.50	0.58	**0.82**
39	C_3H_3	0.2	**0.65**	0.38	**0.61**	**0.89**
41	C_3H_5	0.26	**0.68**	0.48	0.55	**0.80**
43	C_3H_7	**0.11**	0.55	**0.56**	0.59	0.72
43	$C_3H_2O_2$	0.41	**0.63**	0.28	0.35	**0.92**
44	CO_2	**0.64**	0.43	0.35	0.25	0.50
55	C_3H_3O	0.37	**0.70**	0.26	0.45	**0.96**
55	C_4H_7	**0.16**	0.60	**0.59**	0.55	0.73
57	C_4H_9	**0.11**	0.47	0.58	0.57	0.63
57	C_3H_5O	0.34	**0.67**	0.2	0.43	**0.99**
60	$C_2H_4O_2$	0.24	**0.68**	0.27	0.5	**0.99**

Table S3: Correlation table between selected AMS peaks (high resolution m/z) and organic main AMS particle types. Correlations were obtained by temporal series of AMS factor and AMS peaks queries from the dataset.

SI 3. Correlation charts between off-line filter measurements and on-line AMS measurements.

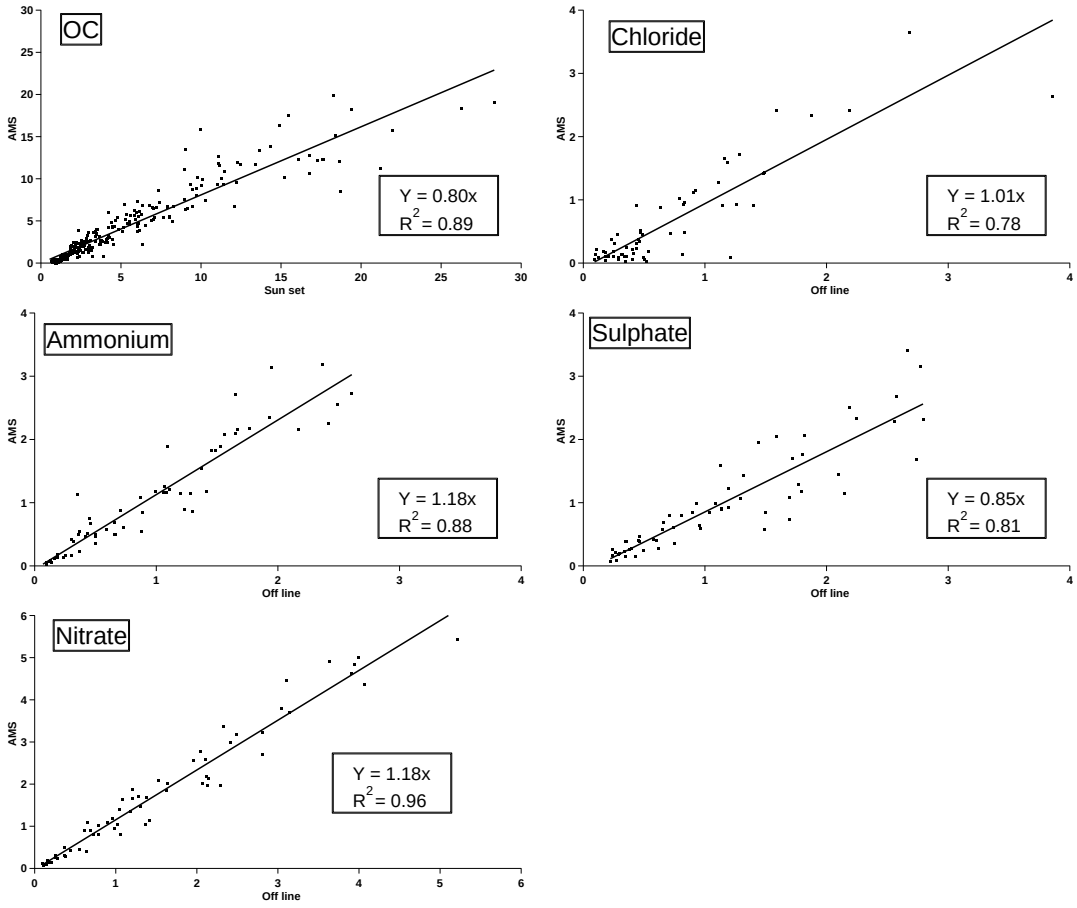

Fig. S2 Correlations between AMS mass and off line techniques ($PM_{2.5}$, all in μg m^{-3}). OM:OC of 1.4 was assumed for converting the AMS organic mass.

SI4. AMS PMF solution description

The PMF analysis on the HR organic matrix of the AMS data was performed for 1 to 6 factors, and summary of diagnostics and results from the different factor solutions is shown in Table S4. PMF solutions with factor numbers greater than 5 provided no new distinct factors and instead displayed splitting behavior of the existing factors.

N Factors	Factors	Note
2	HOA/LV-OOA	HOA has a strong m/z 60
3	HOA/LV-OOA/BBOA	BBOA has a number of peaks not commonly seen in reference spectra, Large residuals at key m/z's and time periods.
4	HOA/LV-OOA/BBOA/PCOA	A new factor PCOA is found.
5	HOA/LV-OOA/BBOA/PCOA/COA	A new factor COA is found. Distinctive diurnal cycles for Factors and MS that compare well with database MS. Better correlation with concomitant measurements (Table S5) than with the 4 factor solution (increase average R^2, see Fig. S5)
>5	Splitting	HOA and LV-OOA begin to split

Table S4. Summary of the AMS PMF results

3.1 Rotational ambiguity

Different 30 seed solutions converged to nearly identical solutions with the lowest value of Q/Qexp (Fig. S3 a). The total range of Q/Qexp varied by only 1% and there were not substantial differences across the 30 solutions (Fig. S3 b). With FPEAK varying from –1 to 0.5 in increment of 0.25 (seed=0), the lowest Q/Qexp was obtained at -0.25 (Q/Qexp = 4.775; (Fig. S3 c-e)) and the total R2 (Table S5) were higher and similar for FPEAK≥–0.25. Therefore, FPEAK=-0.25 was chosen as the best solution.

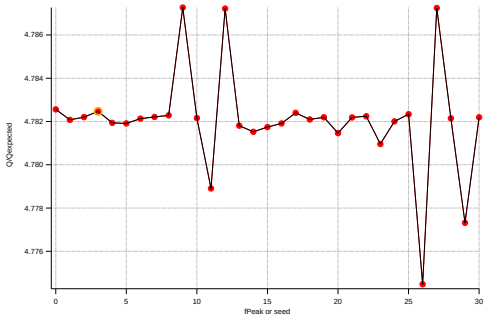

(a)

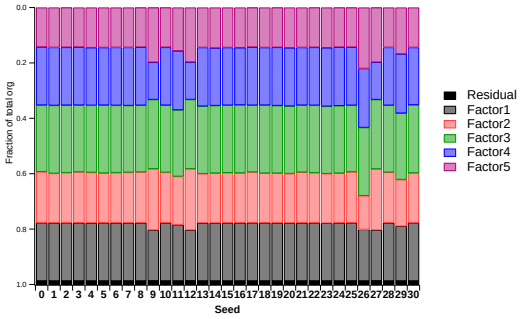

(b)

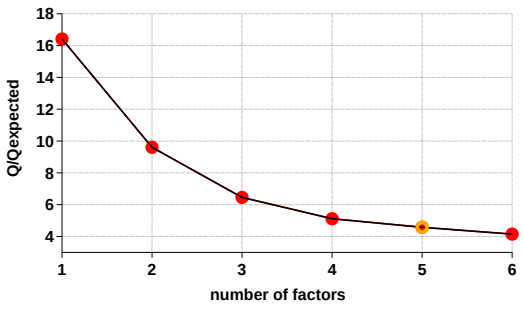

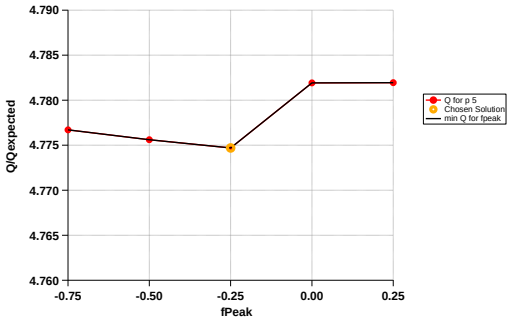

(c) (d)

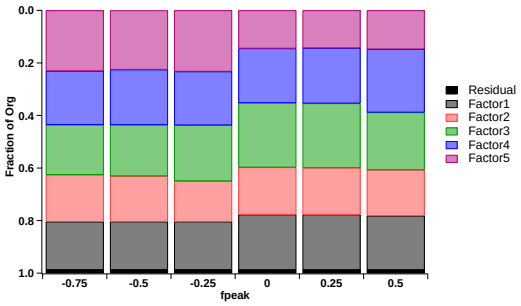

(e)

Fig. S3. PMF rotational ambiguity

In addition, higher correlation values (R^2) between the assigned factors in a PMF solution and their corresponding tracers (in this case gaseous, ATOFMS and off-line filter techniques measurements), were used as additional criterion. Table S5 shows correlation between the 4 and 5 PMF factor solutions and a number of satellite measurements.

1

Solution type		4 factor solution				5 factor solution				
N Factor		1	2	3	4	1	5	3	4	2
Factor name		*LV-OOA*	*BBOA*	*HOA*	*PCOA*	*LV-OOA*	*BBOA*	*HOA*	*PCOA*	*COA*
AMS (1 hour)	**AMS org**	0.22	0.86	0.53	0.77	0.24	0.9	0.43	0.65	0.6
	AMS nit	**0.75**	0.34	0.16	0.1	**0.79**	0.34	0.14	0	0.24
	AMS amm	**0.69**	0.5	0.18	0.23	**0.77**	0.52	0.15	0.17	0.27
	AMS sul	**0.72**	0.22	0.01	0	**0.75**	0.22	0	0	0.15
	AMS Chl	0.29	**0.83**	0.25	0.53	0.38	**0.87**	0.2	0.41	0.4
gas (1 hour)	**NOx**	0	0	**0.31**	0	0	0	**0.39**	0	0
ATOFMS (1 hour)	**OC-EC-SUL**	0	0.23	0.15	0.3	0	0.21	0	0.35	0.22
	OC-EC-NIT	**0.19**	0	0	0	**0.25**	0	0	0	0
	OC-EC-CH	0	0	0	0.25	0	0	0	0.29	0
	Na-K-OC-NIT	**0.57**	0.27	0	0	**0.65**	0.27	0	0	0.33
	Ca-EC	0	0	**0.25**	0	0	0	**0.35**	0	0
Off –Line (6 hours)	**Levoglucosan**	0	**0.75**	0.31	**0.9**	0.16	**0.8**	0.23	**0.84**	0.34
	F	0.15	0.65	0.32	0.7	0.23	0.7	0.25	0.66	0.35
	Cl	0	**0.60**	0.2	**0.77**	0.15	**0.72**	0.17	**0.70**	0.18
	Br	0	**0.66**	0.35	**0.70**	0.12	**0.61**	0.28	**0.75**	0.29
	K	0.21	**0.56**	0.17	**0.59**	0.3	**0.65**	0.11	**0.50**	0.25
Sun set (2 hours)	**EC**	0	0.68	0.38	0.87	0.1	0.72	0.32	0.8	0.35
	OC	0.12	0.53	0.5	0.63	0.15	0.56	0.48	0.58	0.27
	TC	0.1	0.66	0.4	0.8	0.15	0.8	0.37	0.78	0.33

2

Table S5. Correlation table for the four and five PMF solution of the AMS organic matrix and a number of external variables.

All R^2 discussed below are significantly different (at 95% confidence) and the five factor solutions presents, relative to the four factor one:

- HOA increases its correlation with NO_x from 0.31 to 0.39.

- HOA increases its correlation with ATOFMS Ca-EC from 0.25 to 0.35.

- BBOA increases its correlation with AMS Chloride from 0.83 to 0.87, and worse with Br.

- BBOA was found better correlated with levoglucosan, K and Cl at 6 hours resolution.

- LV-OOA shows better correlations between secondary species. Specifically: from 0.75 to 0.79, from 0.69 to 0.77, and from 0.71 to 0.75 for ammonium, sulphate and nitrate, respectively.

- PCOA increases its correlation from 0.3 to 0.35 and from 0.25 to 0.29 of two specific ATOFMS clusters: EC-OC-SUL and EC-OC-CH, respectively. The correlation between these two specific ATOFMS clusters and AMS factor PCOA is unique of this factor.

- PCOA reduced the correlation with biomass markers with a five factor solution, and improve the Br correlation from 0.70 to 0.75.

3.2 Difference between four and five factor solution

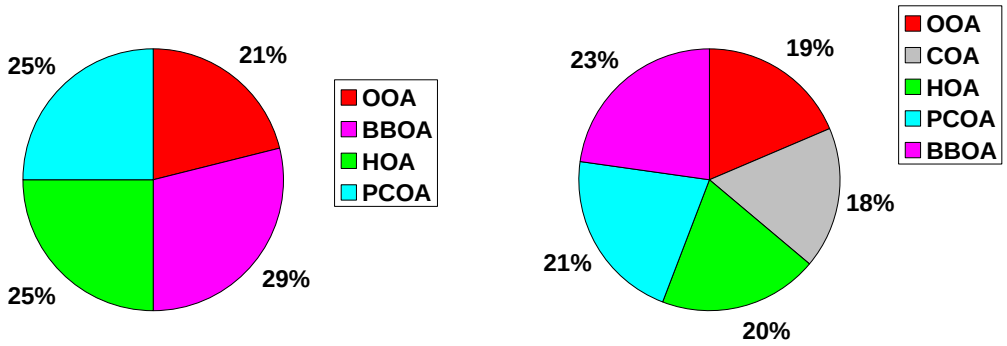

Fig. S4. Average contributions of OA components for the four and five factor PMF solution

PMF Solution	AMS 5 factor					
	Factors	*LV-OOA*	*COA*	*HOA*	*PCOA*	*BBOA*
AMS 4 factor	*LV-OOA*	**0.95**	0.25	0.00	0.00	0.25
	BBOA	0.29	0.65	0.22	0.42	**0.99**
	HOA	0.00	0.46	**0.95**	0.23	0.30
	PCOA	0.1	0.26	0.22	**0.98**	0.61

Table S6. Temporal correlation (as R^2) between four and five factor PMF solutions. PMF factors were found to conserve the temporal trends. The correlation table points out a correlation between BBOA and COA (0.65) , as reported in recent laboratory experiments (He et al. 2010).

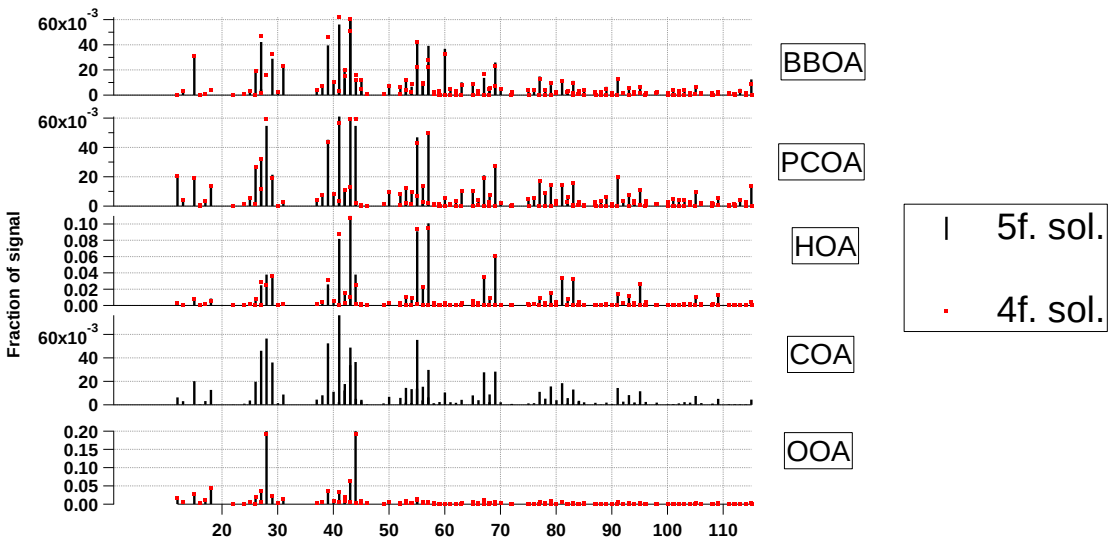

Fig. S5. HRMS of OA components for the four and five PMF factor solution.

3.3 Bootstrapping analysis.

The difficult issue of the uncertainty was also quantitatively addressed with bootstrapping with replacement of MS (Ulbrich et al. 2009, Allan et al. 2010). Fig. S5 shows the mean and standard deviations from bootstrapping along with the base solution. Whilst peak standard deviation of the total signal can be seen for HOA (3.3%) and LV-OOA (7.3%), the other three factors show higher variations: BBOA (20%), PCOA (18%) and COA (21%).

Key peaks for LV-OOA (m/z 28 and m/z 44) as well as for HOA (m/z 43 and 57) shows very low (<2%) peak standard deviations (SD). BBOA shows low peak SD for key marker at m/z 60, but high SD for m/z 57 (29%, tracer for HOA). PCOA shows high SD for peaks at m/z 55 and 57, but lower for key markers such as m/z 39, 41,

44, 77, 91, 113. Finally, COA shows a high SD for m/z 60 (marker for BBOA) and oxidized fraction (m/z 28 and 44), but low SD for key ions (m/z 41, 5%; C_4H_7, 3% and C_3H_3O, 9%).

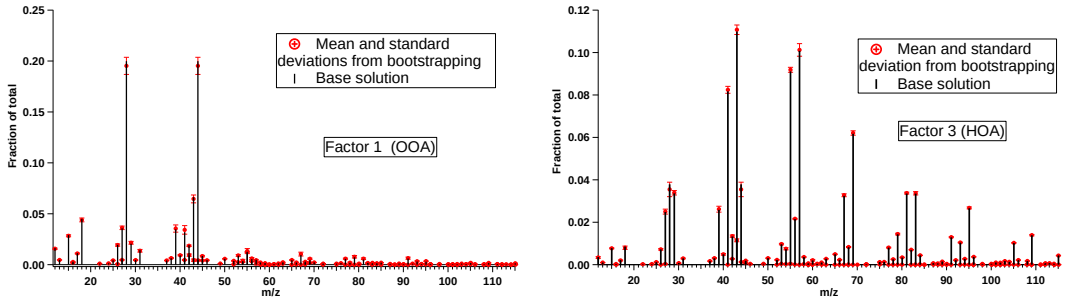

(a)

(b)

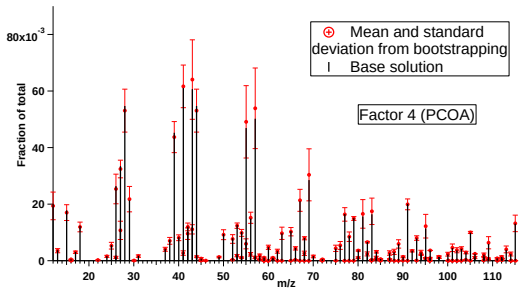

(c)

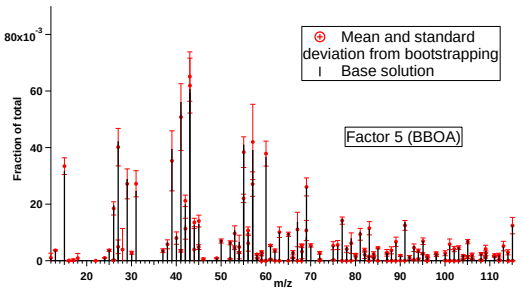

(d)

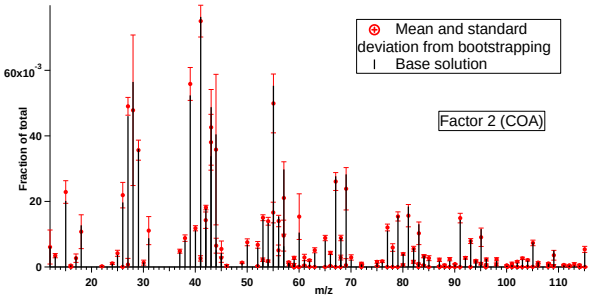

(e)

Fig. S6 a-e. Bootstrapping analysis of the five PMF AMS factor solution.

3.4 Other supporting data

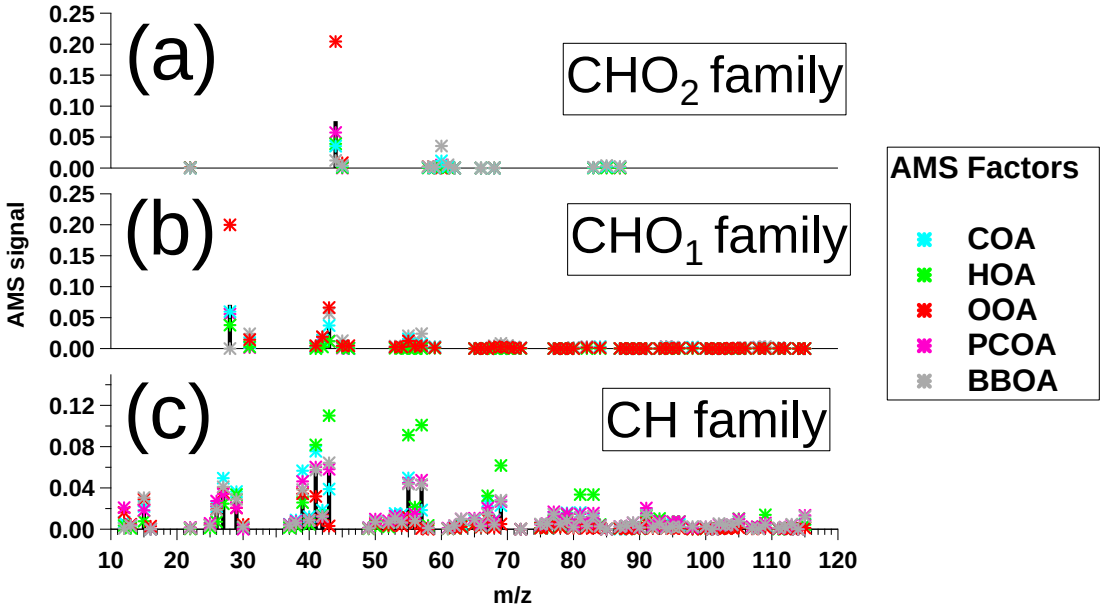

Fig. S7. OA components of the five factor solution separated by the three main ion families: (a) Family CHO_2 as expected is dominated by LV-OOA with m/z 44. Interestingly the second most abundant peak is found at m/z 60 and attributed to BBOA. (b) Family CHO_1 shows again as expected strong signal by LV-OOA at m/z 28 and 43. The peak at m/z 57 (C_3H_5O) is again unique for BBOA. (c) Family CH shows strong signature for HOA. Factor COA shows a different CH patterns with signals at m/z 27, 39, 41 and 55. Finally, m/z 91 for family CH is mainly represented by factor PCOA.

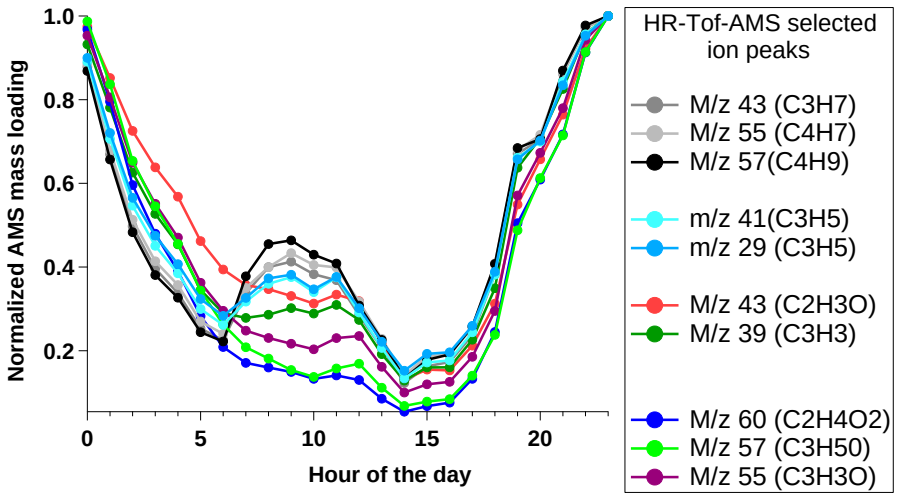

Fig. S8. Diurnal variation of specific HR peaks for the whole period of study. Please note interesting features of m/z 55 (C_3H_3O) and m/z 57 (C_3H_5O) spiking during lunch times but not during traffic conditions, which is capture by the PMF analysis as COA.